Nanoscale

Accepted Manuscript

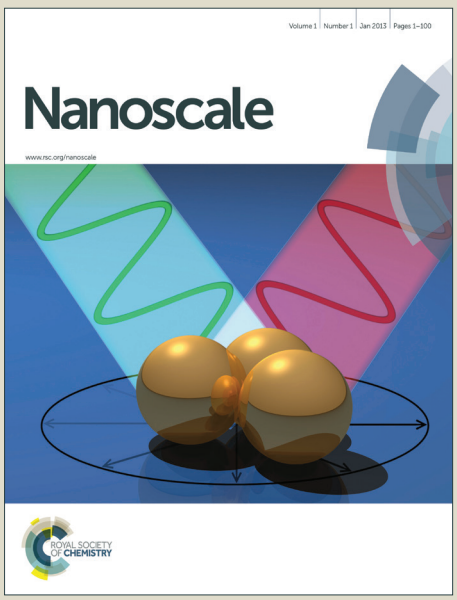

ROYAL SOCIETY OF CHEMISTRY

www.rsc.org/nanoscale

Journal Name

RSCPublishing

ARTICLE

Fast, high-yield synthesis of amphiphilic Ag nanoclusters and the sensing of Hg^{2+} in environmental samples

Nan Xia, [‡a] Jie Yang, [‡a,b] Zhikun Wu*,[a]

Cite this: DOI: 10.1039/xoxxoooooox

Received ooth January 2012,
Accepted ooth January 2012

DOI: 10.1039/xoxxoooooox

www.rsc.org/

We report the high-yield (74%) synthesis of $Ag_{30}(Capt)_{18}$ (abbreviated as Ag_{30}) in a very time-saving fashion (half an hour). The cluster composition was determined by high-resolution mass spectrometry combined with TG analysis, and the structure was probed by 1D and 2D NMR. Interestingly, the nanoclusters can dissolve in water and methanol, as well as in most organic solvents such as ethanol, acetone, acetonitrile, dichloromethane and ethyl acetate with the assistance of acetic acid. Such a good solubility in a range of various polar solvents was not reported previously in nanoclusters research and is important for applications. An important result from this work is that Ag_{30} can sense low concentration of Hg^{2+} in environmental samples (including lake water and soil solution), indicating that Ag_{30} can be a potential colorimetric probe for Hg^{2+}. The sensing mechanism was revealed to be related to the anti-galvanic reduction process.

Introduction

Noble metal nanoclusters (NCs), which bridge the ''missing gap'' between organometallic compounds and nanocrystals, have been very actively investigated in a variety of fields including optics,[1-3] sensing,[4-8] bioimaging,[9-11] biomedicine,[12] and catalysis.[13-17] The size of NCs is close to the Fermi wavelength of an electron (i.e. 0.5 nm for gold and silver), thus the optical, electronic, and chemical properties of NCs are altered sharply with the core size change.[18] On the other hand, the size effect on the percentage of surface atoms and protecting ligands could also affect the properties of NCs.[19] A series of size-discrete, atomically precise gold nanoclusters (AuNCs) protected by thiolates have been reported in recent years, such as Au_{19},[20] Au_{22},[21] Au_{23},[22] Au_{25},[23-25] Au_{30},[26] Au_{36},[27] Au_{38},[28] Au_{55},[29] Au_{67},[30] Au_{102},[31] Au_{130},[32] Au_{144},[33] etc.

Although the growth of AgNCs is lagged behind the prosperous gold analogues owing to its susceptibility to oxidation and aggregation,[34] AgNCs are finding ever-expanding roles in many areas due to high surface-to-volume ratio, facile surface tailorability, and desirable luminescence properties.[35] Several stabilizers were introduced for AgNCs, such as dendrimers, polyelectrolytes, DNA, proteins, and small molecules containing carboxylic groups or thiols.[36] A limited number of thiolate-protected AgNCs with well-defined chemical composition such as Ag_7,[37] $Ag_{7,8}$,[38] Ag_9,[39] Ag_{15},[40] Ag_{16},[41] Ag_{31}[40], Ag_{32},[42, 43] and Ag_{44}[34] have been prepared until now. Of note, among them, the crystal structure of Ag_{44} has been attained recently and the staple motif on Ag_{44} surface is totally different from the case of gold nanoclusters (Ag_{14},[44] Ag_{16},[45] Ag_{32},[45] Ag_{62},[46, 47] Ag_{70},[48] Ag_{262},[48] Ag_{320},[49] and Ag_{490}[49] are not considered herein due to their complicated surface protecting). Those fundamental scientific issues involving structures and properties stimulate enormous interests in a wide range of fields, from solid-state physics to chemistry and nanotechnology very recently. However, the research on silver nanoclusters was seriously hampered by the synthesis and identification difficulties, thus, the development of new synthesis strategy is of major importance. It is known that some other nanomaterials [50, 51] as well as silver nanoclusters[4, 52-54] exhibit potential as fluorescent probes. Although AuNP-based colorimetric assays[55] and colorimetric response of few-atom silver nanoclusters to organics[56] have been previously reported, however, silver nanocluster as colorimetric ion probes have not been reported by now to the best of our knowledge. The development of colorimetric silver nanocluster probes should be preferentially considered, given lots of virtues of this analytical method such as the operation facility and simplicity, high accuracy and reproducibility, and low cost and easy miniaturization of UV/vis/NIR absorption spectrophotometer.[5]

In this work, we present a fast (30 min), high-yield synthesis of silver nanoclusters protected by captopril. The nanoclusters are well-defined based upon characterization by UV/vis/NIR absorption spectrometry, polyacrylamide gel electrophoresis (PAGE), electrospray ionization mass spectrometry (ESI-MS), thermal gravimetric analysis (TGA) etc. A very interesting finding is the good solubility of silver nanoclusters in a wide range of solvents, which is of great importance for application and has not been reported previously in nanocluster research to the best of our knowledge.

promising application related to the as-prepared silver nanoclusters is the selective and sensitive sensing of notorious Hg^{2+}. Even ~6 ppb levels of mercury in environmental samples (for instance, lake water) can be detected, indicating the potential of Ag_{30} nanoclusters as a colorimetric probe. The sensing mechanism was also investigated.

Experimental

Synthesis

The synthesis of $Ag_{30}Capt_{18}$ was carried out at room temperature under air. First, $AgNO_3$ (85 mg, 0.50 mmol) was dissolved in 25 ml deionized water, and captopril (141 mg, 0.65 mmol) was added, forming a yellow-green solution. Then, NaOH (55 mg, 1.38 mmol) was added to adjust the pH value to ~11. The stirring speed was ~500 rpm. Then a freshly made 5 ml aqueous solution of $NaBH_4$ (189 mg, 5.00 mmol) was slowly added dropwise. The solution gradually turned from pale green to dark green, and finally deep brown. The reaction was allowed to age for 25 min. The crude clusters were precipitated by 3-fold ethanol. Further purification was carried out by extracting the precipitate with minimum amounts of water 3~4 times and precipitating again by ethanol.

Characterization

High-resolution transmission electron microscopy (HR-TEM) images were recorded using an electron microscope operated at 200 kV (JEM-2010). Electrospray ionization (ESI) mass spectrometry (ESI-MS) was performed using a Waters Q-TOF mass spectrometer equipped with a Z-spray source. UV-Vis absorption spectra of the clusters were recorded in water at the ambient temperature on a UV/Vis/NIR spectrophotometer (Shimadzu, UV2550). Thermal gravimetric analysis (TGA) (~ 3 mg sample used) was conducted in a N_2 atmosphere (flow rate ~ 50 mL/min) on a TG/DTA 6300 analyzer (Seiko Instruments, Inc), and the heating rate was 10 ^oC /min. ^1H, HSQC, COSY NMR spectra of AgNCs were recorded in D_2O with concentration of 5.7 wt % at 27 ^oC on a Buker Avance 400 NMR spectrometer. Polyacrylamide gel electrophoresis (PAGE) in acrylamide gels (15%, 20%, 25% monomer and 5% cross-linker) in a tris(hydroxymethyl)aminomethane base buffer of a pH~8 was used for AgNC purity monitoring.

Colorimetric Detection

Ultrapure water was used as received. The lake water was taken from Shushan lake near Heifei city on September 22, 2014 and was filtrated through a membrane filter (0.22 μm) prior to use. The soil was obtained from west dwelling district of Kexue island in Hefei on September 22, 2014. Soil solution was prepared as follows: first, soil sample was heated in an oven at 80 ^oC for one hour, secondly, 1 g of the dried soil sample was weighted into a vial and mixed with 8 ml of 1 M aqua regia. After ultrasonication for 10 min, the resulting extracts were centrifuged and diluted 100 times using ultrapure water, then tune the pH value to ~10, finally filtered using 0.22 μm membrane.[58]

The pH values of all the samples with various cations were adjusted to ~10. Then the concentrated Ag_{30} solution was added into the analyte sample with a final concentration of 3.0 μM. The aqueous solutions of Ag nanoclusters and Hg^{2+} with different concentrations were mixed, then equilibrated for 10 min before the spectral measurements. The mixed cation samples were prepared using 20 mM salt stock solutions.

Results and discussion

Synthesis and Characterization

The present approach to prepare AgNCs is very facile (detail in the Experimental Section) and similar to the previous reports.[59, 60] Briefly, in a freshly prepared water solution of $AgNO_3$ and captopril, appropriate amount of NaOH was added to tune the pH value to ~11. $NaBH_4$ dissolved in ice cold water was slowly added to the aqua mixture under vigorous stirring. After ~15 min, the characteristic optical absorption peaks of silver nanoclusters appeared and reinforced in the next 10 min (Fig. S1). Then the clusters were precipitated out by 3-fold (volume) ethanol. The crude product was subjected to purification by recrystallization in EtOH/H_2O for 3-4 times. The purity of the product was evaluated by polyacrylamide gel electrophoresis (PAGE) analysis. The crude product shows at least two major bands (one brown band and one pale yellow band, see Fig. 1(a)), indicating the existence of impurities (Fig. 1 A, inset a), while the purified clusters show only one well-defined band in different operation conditions (Fig. 1 B and C), indicating a higher purity. The reaction can be readily scaled up, and we obtained ~1.0 g pure clusters by a 10 times scale-up with a yield of 74%.

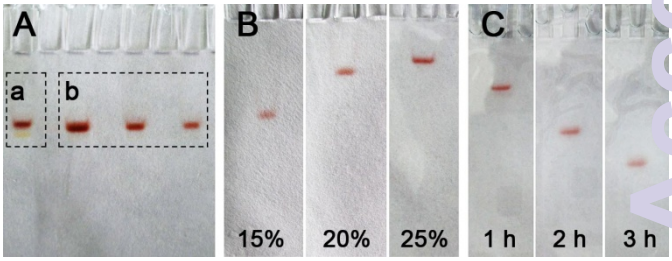

Fig. 1 (A) PAGE analysis of the crude Ag clusters (a) and purified Ag clusters (b) with increasing loading amount of Ag clusters from right to left; PAGE analysis of the purified Ag clusters in acrylamide gels with different monomer concentrations (B) and running times (C).

As we know, the thiolate (ligand) plays an important role in protecting silver nanoclusters. Thereby, the stability of the ligand needs to be primarily taken into consideration in the design of novel nanocluster synthesis. Glutathione, a multidendate ligand, was regarded to be a good stabilizer and widely used to protect gold or silver nanoclusters.[61] Nevertheless, Kumar et al. recently reported that glutathione-protected Au_{25} exhibits somewhat less thermal stability compared to the captopril-protected Au_{25}, which indicates that captopril may be a better protecting ligand for metal clusters.[62] Besides, captopril is an effective Angiotensin-I converting

enzyme (ACE) inhibitor and has been widely employed to treat high blood pressure, congestive heart failure, and cardiovascular disease.[63] Another favorable property of captopril involves the good solubility in various solvents. Thus, employing captopril as the protecting ligand to prepare silver nanoclusters could be a good choice.

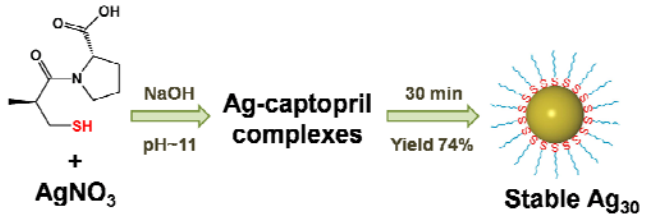

Fig. 2 Schematic illustration of the postulated formation of $Ag_{30}(Capt)_{18}$ NCs.

The tuning of pH value of the reaction mixture before the addition of $NaBH_4$ is very important in this reaction, too, which influences the kinetics of the reaction by slowing the reducing of $NaBH_4$ and strengthening the binding of Au-thiolate.[20, 64] The reaction temperature can influence reaction rate greatly: At 0 °C, the reaction took about 6 hours to achieve the yield of ~74%; while at room temperature, the reaction can be completed in ~30 min as stated above. Higher temperature (e.g. 40 °C) contributes little to further improvement of the yield. Thus room temperature is adopted for this reaction. One remarkable virtue of this synthesis method compared with previous size-focusing processes[20] is the very short reaction time (30 min), due to that the as-prepared clusters is both kinetically and thermodynamically favorable. Other virtues like high purity and high yield (74%) are attractive not only for research purposes but also for practical applications. The summary of the synthesis information in this work and some reported work is showed in Table S1. Compared with the previously reported methods, our strategy offers facile operation (carried out at room temperature under air), short time (30min) and good yield (74%) for the synthesis of silver nanoclusters.

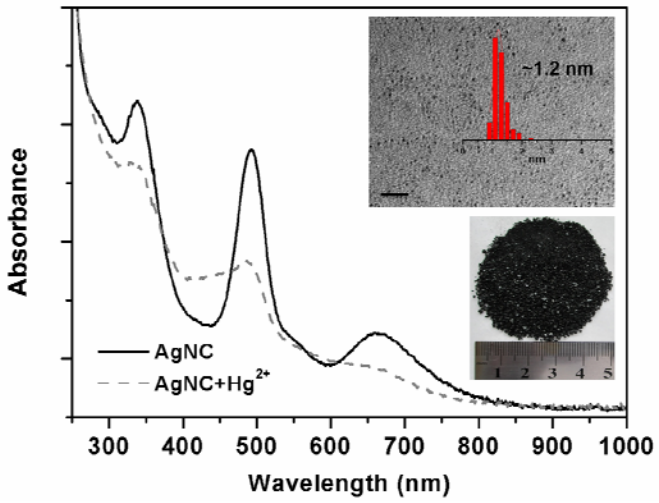

Fig. 3 UV/vis/NIR spectrum of the pure product in water (solid line) and in the presence of 2 μM Hg^{2+} (dash line), inset shows the TEM image of Ag clusters (scale bar = 20 nm) and the photo of 1.0 g Ag nanoclusters and the ruler.

The aqueous solution of the as-prepared captopril-protected Ag clusters exhibits three prominent peaks (335 nm, 493nm, 660 nm) and three shallow peaks (215nm, 415nm, 550nm) in UV/vis/NIR spectrum[59, 60] (Fig. 3). The clusters appeared as tiny dots in the transmission electron microscopy (TEM) image (inset in Fig. 3 and Fig. S2), with a uniform size of ca. 1.2 nm, which aggregate to form nanoparticles (2~5 nm) after longer time of electron beam irradiation.

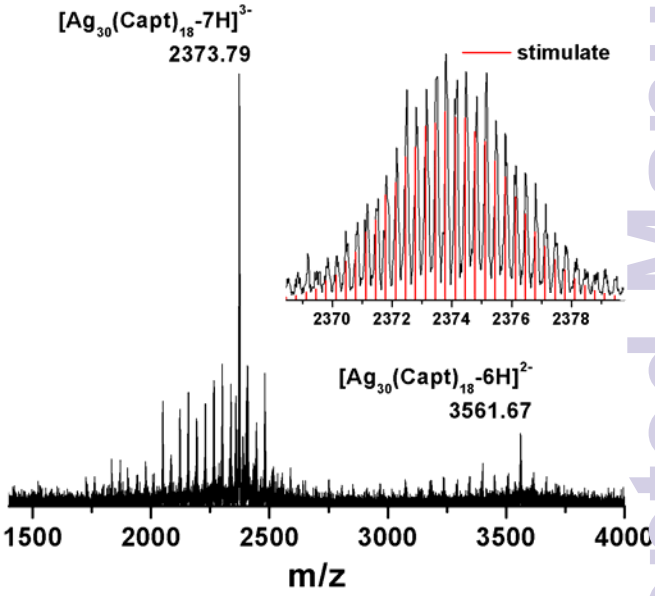

Fig. 4 ESI mass spectra (in negative ion mode) of the as-prepared silver nanoclusters, inset shows the isotope patterns of $[Ag_{30}(Capt)_{18}\text{-}7H]^{3-}$.

The precise composition determination is very challenging due to the unstability of silver nanoclusters. Besides, the isotopic distributions are complicated significantly by the two abundant naturally occurring silver isotopes, ^{107}Ag and ^{109}Ag, in addition to carbon and sulfur isotopes. By now, only a few nanoclusters have been precisely characterized by high-resolution mass spectrometry. Fortunately, in this work, the silver cluster is successfully identified by electrospray ionization mass spectrometry (ESI-MS) partly due to the stability of the as-prepared nanoclusters. In the ESI-MS spectrum, the most abundant peak is found at m/z 2373.79 Da and the spacing (0.33 Da) of the isotope peaks indicates that the ionized cluster bears a 3- charge. It can be readily assigned to the formula $[Ag_{30}(Capt)_{18}\text{-}7H]^{3-}$ (expected: 2373.78 Da; deviation: 0.01 Da; Capt represents the thiolate form of captopril) based on the high performance of our MS facility (error < 5 ppm at M/Z = 1000, external calibration). 7 protons rather than other numbered protons from the mother ion is lost, may due to the stability of the eight-electron shell closing structure of $[Ag_{30}(Capt)_{18}\text{-}7H]^{3-}$ ($n^*=Nv_A-M-Z=32*1-18-(7-3)=8$).[65, 66] The assignment is further supported by the excellent

agreement of the simulated and experimental isotopic distributions (Fig. 4, inset), together with the detecting of a distinct peak at *M*/*Z* 3561.67 assigned to $[Ag_{30}(Capt)_{18}\text{-}6H]^{2-}$ (for the comparison between simulated and experimental isotopic distributions, see Fig. S3). Thermogravimetric analysis (TGA) provides another support for the assignment: A weight loss of 54.0 wt % is consistent with the value expected for a formula of $Ag_{30}(Capt)_{18}$ (54.6 wt %) (see Fig. S4). To be noted, slight fragmentation or adduction of the mother ion are also found around the base peak, and they can be well assigned (Table S2).

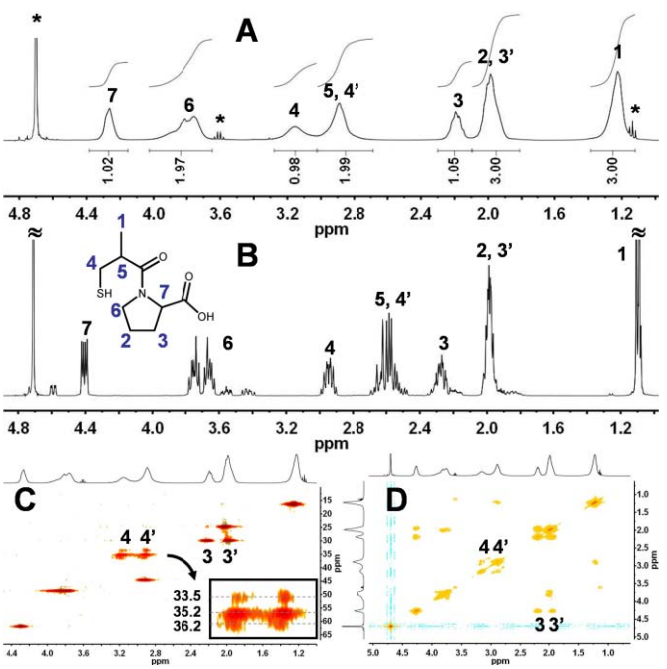

Fig. 5 ^{1}H NMR spectra of $Ag_{30}(Capt)_{18}$ nanoclusters (A) (peaks marked with * at 3.6 ppm and 1.1 ppm are due to residual EtOH) and free captopril (B), HSQC spectrum (inset shows the enlarged pattern of [4, 4'] split) (C) and COSY spectrum (D) of $Ag_{30}(Capt)_{18}$ nanoclusters. Solvent: D_2O.

The atomic packing structures of thiolated silver nanoclusters, as opposed to gold analogues, are rarely known. For mono-thiolated silver nanoclusters, the structure of Ag_{44} was recently unravelled by Desireddy et al.[34] Single crystal structure of of $Ag_{30}(Capt)_{18}$ (abbreviated as Ag_{30}) is still not attained until now due to the difficulty in growing high-qualified single crystals for X-ray diffraction analysis. Nuclear magnetic resonance (NMR) spectroscopy, which provides important structure information in our previous work,[67] is employed to probe the nature of the staple motif on the cluster surface. First, the protons were fully assigned based on the 1D NMR and homonuclear correlation spectroscopy (COSY), see Fig. 5A, B and D (for convenience, the carbon atoms in captopril are labeled with numbers 1-7 from upfield to downfield). Note that the chiral carbons C5 and C7 cause the splitting of H_4 and H_3 signals, respectively. Herein, H_4 is the focus of attention since it is adjacent thus sensitive to Ag-S binding. Interestingly, the chirality-induced splitting [4, 4'] is further divided into three pairs of peaks connected to three different carbon atoms (33.5 ppm, 35.2 ppm and 36.2 ppm, respectively) in heteronuclear single quantum correlation (HSQC) spectrum, see Fig. 5C, which indicates that there are three types of chemically distinct thiolate-silver binding mode. To be noted, the three pairs of peaks are overlapped and barely discernible in 1D NMR and 2D COSY, thus it is difficult to know the quantitative ratio of the peak areas. Nevertheless, the qualitative determination of the three pairs of the peaks provides important information to conceive the staple motif type on the cluster surface. Definitely, the complete $–[RS_a–Ag–S_b(R)–Ag–S_aR]–$ staple can be ruled out since it will result in two pairs of peaks in 2:1 ratio for $–S_aR$ and $–S_bR$, as analyzed in our previous report;[67] the monomeric $–[RS_a–Ag–S_a(R)]$ staple can also be ruled out, since it would result in only one pair of peaks. The novel staple type $Ag_2(SR)_5$ found in Ag_{44} is also impossible since it would lead to three pairs of peaks in a 1:2:2 ratio (in our case, the ratio is roughly 1:2:1 from the HSQC spectrum); other complete staple types like $Ag_3(SR)_4$, $Ag_4(SR)_5$, $Ag_5(SR)_6$ can also be excluded due to all of them would produce splits distinctly different from the experimental results in this work. One possibility is a combination of different staple types, for instance, a combination of $–[RS_a–Ag–S_aR]–$ and $–[RS_a–Ag–S_bR–Ag–S_aR]–$ staples. Of course, there are other possibilities. For the exact structure, it remains to be determined in future work.

Table 1. Solubility of Ag_{30} in various solvents (acetic acid 20% by volume, 25°C)

Solvent	Solubility (g/L)	Description
water [a]	≥1000	Excellent
Methanol [a]	31.3	Good
ethanol	28.8	Good
propanol	20.8	Good
butanol	22.4	Good
DCM	20.0	Good
chloroform	24.0	Good
acetonitrile	3.6	Good
toluene	0.8	Poor
acetone	4.0	Good
THF	8.0	Good
dioxane	5.6	Good
ethyl acetate	0.5	Poor
DMF	19.2	Good
DMSO	95.6	Excellent

[a] no addition of acetic acid

Solubility performance

The solubility of nanocluster is of importance for characterization and potential application in a range of fields such as biomedicine and catalysis. Desireddy et al have reported that water-soluble Ag_{44} can be transformed to DMF after protonation with acetic acid. Herein, we found that the freshly prepared Ag_{30} can only dissolve in fewer solvents such as water and methanol, however, the protonation of the carboxylate (e.g., by 10% v/v acetic acid) greatly enhances the solubility, and leads to good dispersion of Ag_{30} in a large range of solvents of various polarity such as ethanol, acetone,

acetonitrile, dichloromethane and ethyl acetate. The solubility change process is showed in Fig. S5. For the summary of the solubility of Ag_{30} in various solvents, see Table 1. The dispersion of Ag_{30} in various solvents is attributed to the excellent solubility of protonated captopril ligands. It is well known that water-soluble NPs/NCs facilitate their application in biological and medical fields, while the addition of hydrophobic feature to NPs/NCs allows for the superior penetration through the cellular membrane and nuclear pores.[68-70] Another promoting aspect of NPs/NCs derived from their solubility is catalysis. More reactions in various solvent systems can be catalyzed by the NPs or NCs with universal solubility.[71, 72] In a word, the good solubility of Ag_{30} will be greatly beneficial to their applications, and some of the related research are underway in our group.

Colorimetric Detection of Hg^{2+}

The interesting solubility and molecule-like UV/vis/NIR absorption remind one that it may be employed as a colorimetric probe for heavy metal ions. Hg^{2+} receives extensive attention due to its high toxicity and wide-range contamination in environment.[57] Thus, we have primarily investigated the possibility of sensing Hg^{2+} by Ag_{30}. Indeed, the addition of Hg^{2+} instantly (a couple of seconds) shows effects in the UV/vis/NIR spectrum of Ag_{30}, even trace Hg^{2+} can lead to a notable decrease of the absorbance, see Fig. 3 and Fig.S6.

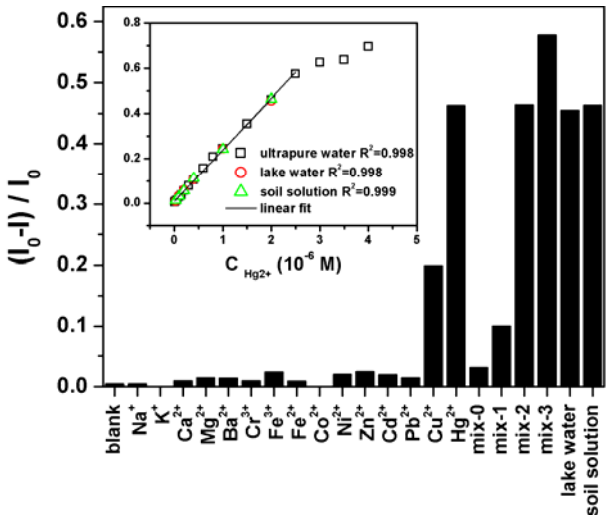

Fig. 6 Absorbance response at 493 nm of Ag_{30} to various cations. The bars represent the $(I_0-I)/I_0$ values: blank, without any analyte cations; Na^+ to Hg^{2+}, 2 μM for each cation; mix-0: mixed ions, 10 μM for each cation; mix-1: mixed ions + Cu^{2+}, 2 μM for Cu^{2+} and 10 μM for each other cation; mix-2: mixed ions + Hg^{2+}, 2 μM for Hg^{2+} and 10 μM for each other cation; mix-3 mixed ions + Hg^{2+} + Cu^{2+}, 2 μM for each cation. The inset shows a plot of $(I_0-I)/I_0$ versus the concentration of Hg^{2+}. (Mixed ions includes these cations: Na^+, K^+, Ca^{2+}, Mg^{2+}, Ba^{2+}, Cr^{3+}, Fe^{3+}, Fe^{2+}, Co^{2+}, Ni^{2+}, Zn^{2+}, Cd^{2+}, Pb^{2+}).

A systematic study reveals that the concentration of Hg^{2+} is linear with the intensity ratio I_0/I in a wide concentration range from 10 nM to 2.5 μM, see Fig. 6 inset. Herein, I_0 represents the initial absorbance of Ag_{30} solution at 493 nm (corresponding to the maximum absorption peak), and I represents the absorbance after the addition of Hg^{2+}. The detection limit is as low as 30 nM based on the formula: $S_t - S_b \geq K_d\sigma$(S_t is the analyte signal, S_b is the blank signal, a value of 3 for K_d is recommended, σ is the standard deviation of the blank sample).[73] To investigate the selectivity of Ag_{30} to Hg^{2+}, various metal ions were tested. It is found that the addition of other 13 metal ions (including Na^+, K^+, Ca^{2+}, Mg^{2+}, Ba^{2+}, Cr^{3+}, Fe^{3+}, Fe^{2+}, Co^{2+}, Ni^{2+}, Zn^{2+}, Cd^{2+} and Pb^{2+}, 2 μM) results in negligible or only slight change of the absorbance, even the coexistence of the 13 metal ions in higher concentration (10 μM for each cation) only causes a less than 3% decrease of I_0, in striking contrast to the case of Hg^{2+} (46% decrease, for a lower concentration 2 μM). Interestingly, the coexistence of all the other 13 metal ions (10 μM for each cation) doesn't interfere with the detection of Hg^{2+} (2 μM) at all, see Fig. 6 and Fig. S7. These results demonstrate that Ag_{30} has excellent selectivity to Hg^{2+} over the above investigated metal cations.

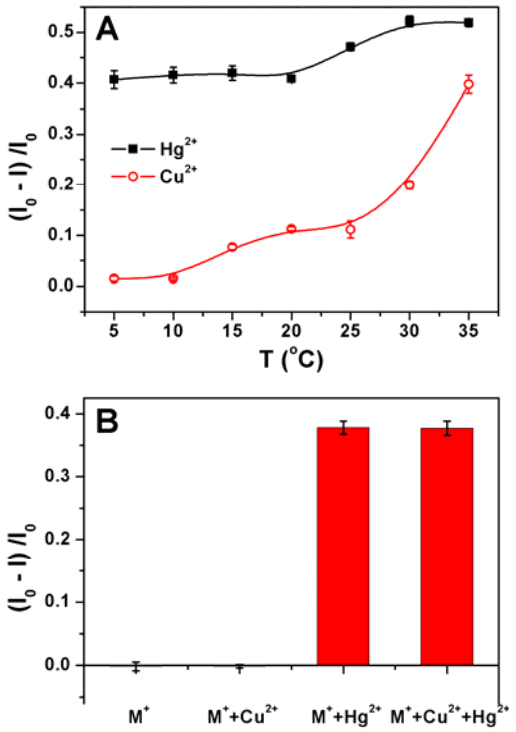

Fig. 7 (A) Absorbance response at 493 nm of Ag_{30} to Hg^{2+} and Cu^{2+} with changing incubation temperature. (B) Absorbance response at 493 nm of Ag_{30} to mixed ions at 10°C. M^+: mixed ions includes Na^+, K^+, Ca^{2+}, Mg^{2+}, Ba^{2+}, Cr^{3+}, Fe^{3+}, Fe^{2+}, Co^{2+}, Ni^{2+}, Zn^{2+}, Cd^{2+}, Pb^{2+}; M^+ + Cu^{2+}: 2 μM for Cu^{2+} and 10 μM for each other cation; M^+ + Hg^{2+}: 2 μM for Hg^{2+} and 10 μM for each other cation; M^+ + Cu^{2+} + Hg^{2+}: 2 μM for Cu^{2+}, Hg^{2+} and 10 μM for each other cation

However, the co-existence of free Cu^{2+} (i.e. without masking) has some interfere to the accurate determination of Hg^{2+} concentration, see mix-3 in Fig. 6. Interestingly, lowering the incubation temperature can remarkably improve the selectivity of Ag_{30} to Hg^{2+} due to that the sensing of Cu^{2+} (compared with Hg^{2+}) are less sensitive in low temperature. For instance, in 10 °C, detectable change of absorption of Ag_{30} was not observed when exposed to 2μM of Cu^{2+}. A systematical comparison between Hg^{2+} and Cu^{2+} among the temperature

range from 5 to 35°C was presented in Fig. 7A. At low temperature, other ions also have no interference to the sensing of Hg^{2+} by Ag_{30}, see Fig. 7B. Therefore, Ag_{30} can selectively sense Hg^{2+} even in the presence of Cu^{2+} and other mentioned cations under low temperature (e.g. 10 °C). Herein, the low-temperature masking (LTM) method, which is not reported previously to our best knowledge, is rather facile and could be extended to other sensing systems for the masking of temperature-dependent interference. The compositions of practical environmental samples are far more complex than that of mixed ions. The sensing of Hg^{2+} in environmental samples (including lake water and soil solution) was investigated and it is surprisingly found that the colorimetric probe can be applied in detecting low concentrate Hg^{2+} down to 30 nM (6 ppb) (with a deviation of 6.2%) in lake water, see Fig. 6 and S8, indicating the great potential of Ag_{30} for practical assay of Hg^{2+}. To be noted, dramatic measurement deviations for the same sample (6 ppb Hg^{2+} in lake water) were found when employing some conventional methods (2600% deviation for atomic fluorescence spectrometry(AFS); 62% deviation for inductively coupled plasma mass spectrometry (ICP-MS)).

A question naturally arising is what the sensing mechanism is. The fact that the addition of ethylene diamine tetraacetic acid (EDTA) does not lead to the recovery of absorbance of Ag_{30} (see Fig. S9 and S10) excludes the possible binding of Hg^{2+} with the ligands or silver core of Ag_{30}. The intrinsic mechanism may be related to the recently reported anti-galvanic reduction (AGR).[74-76]. During the process of ion detection, Hg^{2+} (or Cu^{2+}) can oxidize Ag_{30}, thus resulting in the decrease of absorbance; while the other investigated metal cations can not due to the limited oxidation capability (several standard reduction potential of M^{x+}/ M^{y+}(x>y) in alkaline solution are showed as follows: Hg^{2+}/Hg, 0.0977 V; Cu^{2+}/Cu^{+}, -0.080 V; Fe^{3+}/Fe^{2+}, -0.56 V; Pb^{2+}/Pb, -0.580 V; Ni^{2+}/Ni, -0.72 V; etc[77]). Indeed, the XPS analyses revealed that Hg^{2+} and Cu^{2+} (unlike Ni^{2+} and Pb^{2+}) were reduced after mixed with Ag_{30} in 30 °C (Fig. S11). The temperature-dependent response of Ag_{30} to Cu^{2+} can also be well explained by the sensing mechanism, that is, the oxidation-reduction between Ag_{30} and Cu^{2+} is temperature-dependent and proceeds slowly (or difficultly) at low temperature due to the weak oxidability of Cu^{2+} compared with that of Hg^{2+}. The facts that other common oxidants such as H_2O_2 and $KMnO_4$ can cause the prompt decrease of Ag_{30} absorbance at 493 nm also provide evidences for such a mechanism (Fig. S12). The almost unchanged size of Ag_{30} after reaction with Hg^{2+} excludes the possibility of Hg^{2+}-induced aggregation or discomposing of Ag_{30} (Fig. S13).

Conclusions

In summary, we have succeeded in fast (30 minutes), high-yield (74%) synthesis of $Ag_{30}(Capt)_{18}$. The composition was precisely determined by ESI-MS, and the structure was probed by 1D and 2D NMR. One interesting finding is that the clusters after protonation can dissolve in water and a large range of organic solvents with various polarity such as ethanol, acetone, acetonitrile, dichloromethane and ethyl acetate. Such a property imparts $Ag_{30}(Capt)_{18}$ a great merit for potential application. Very importantly, by sensing ~6 ppb levels of Hg^{2+} in the environmental samples it is demonstrated that Ag_{30} can be a potential colorimetric probe for Hg^{2+}. For the first time, a LTM method was developed to mask the interference from other cations. The sensing mechanism is confirmed to be related to the anti-galvanic reduction. Our present study represents a significant step forward in the synthesis and application of atom-precise silver nanoclusters and will provide some references for the future research and practical applications of silver nanoclusters.

Acknowledgements

Z.W. would like to thank National Basic Research Program of China (Grant No. 2013CB934302), the Natural Science Foundation of China (No. 21222301, 21171170), the Ministry of Human Resources and Social Security of China, the CAS/SAFEA International Partnership Program for Creative Research Teams and the Hundred Talents Program of the Chinese Academy of Sciences for financial support.

Notes and references

[a] Key Laboratory of Materials Physics, Anhui Key Laboratory of Nanomaterials and Nanotechnology, Institute of Solid State Physics, Chinese Academy of Sciences (CAS), Hefei 230031, Anhui, China. E-mail: zkwu@issp.ac.cn

[b] Department of Chemistry, University of Science and Technology of China, Hefei, Anhui 230026, China

‡ N. Xia and J. Yang contributed equally

† Electronic Supplementary Information (ESI) available. See DOI: 10.1039/b000000x/

1 H. Zhang, D. E. Zelmon, L. G. Deng, H. K. Liu and B. K. Teo, *J. Am. Chem. Soc.*, 2001, **123**, 11300-11301.

2 J. Zheng, C. Zhang and R. M. Dickson, *Phys. Rev. Lett.*, 2004, **93**, 077402.

3 N. Sakai and T. Tatsuma, *Adv. Mater.*, 2010, **22**, 3185-3188.

4 W. Guo, J. Yuan and E. Wang, *Chem. Commun.*, 2009, 3395-3397.

5 J. P. Xie, Y. G. Zheng and J. Y. Ying, *Chem. Commun.*, 2010, **46**, 961-963.

6 S. W. Yang and T. Vosch, *Anal. Chem.*, 2011, **83**, 6935-6939.

7 Z. K. Wu, M. Wang, J. Yang, X. H. Zheng, W. P. Cai, G. W. Meng, H. F. Qian, H. M. Wang and R. C. Jin, *Small*, 2012, **8**, 2028-2035.

8 X. Wu, R. Li, Z. Li, J. Liu, G. Wang and Z. Gu, *RSC Adv.*, 2014, **4**, 24978-24985..

9 J. Yu, S. A. Patel and R. M. Dickson, *Angew. Chem. Int. Ed.*, 2007, **46**, 2028-2030.

10 L. Shang, N. Azadfar, F. Stockmar, W. Send, V. Trouillet, M. Bruns, D. Gerthsen and G. U. Nienhaus, *Small*, 2011, **7**, 2614-2620.

11 L. Zhang, J. Zhu, Z. Zhou, S. Guo, J. Li, S. Dong and E. Wang, *Chem. Sci.*, 2013, **4**, 4004-4010.

12 M. C. Bowman, T. E. Ballard, C. J. Ackerson, D. L. Feldheim, D. M. Margolis and C. Melander, *J. Am. Chem. Soc.*, 2008, **130**, 6896-6897.

13 N. K. Chaki, H. Tsunoyama, Y. Negishi, H. Sakurai and T. Tsukuda, *J. Phys. Chem. C* 2007, **111**, 4885-4888.
14 W. Chen and S. Chen, *Angew. Chem. Int. Ed.,* 2009, **48**, 4386-4389.
15 Y. Zhu, H. Qian, B. A. Drake and R. Jin, *Angew. Chem. Int. Ed.,* 2010, **49**, 1295-1298.
16 M.-B. Li, S.-K. Tian and Z. Wu, *Nanoscale*, 2014, **6**, 5714-5717.
17 D. R. Kauffman, D. Alfonso, C. Matranga, P. Ohodnicki, X. Deng, R. C. Siva, C. Zeng and R. Jin, *Chem. Sci.*, 2014, **5**, 3151-3157.
18 J. Zheng, P. R. Nicovich and R. M. Dickson, *Annu. Rev. Phys. Chem.,* 2007, **58**, 409-431.
19 Y. Z. Lu and W. Chen, *Chem. Soc. Rev.,* 2012, **41**, 3594-3623.
20 Z. Wu, M. A. MacDonald, J. Chen, P. Zhang and R. Jin, *J. Am. Chem. Soc.,* 2011, **133**, 9670-9673.
21 J. Chen, Q.-F. Zhang, T. A. Bonaccorso, P. G. Williard and L.-S. Wang, *J. Am. Chem. Soc.,* 2013, **136**, 92-95.
22 A. Das, T. Li, K. Nobusada, C. Zeng, N. L. Rosi and R. Jin, *J. Am. Chem. Soc.,* 2013, **135**, 18264-18267.
23 Y. Shichibu, Y. Negishi, T. Tsukuda and T. Teranishi, *J. Am. Chem. Soc.,* 2005, **127**, 13464-13465.
24 M. W. Heaven, A. Dass, P. S. White, K. M. Holt and R. W. Murray, *J. Am. Chem. Soc.,* 2008, **130**, 3754-3755.
25 M. Zhu, C. M. Aikens, F. J. Hollander, G. C. Schatz and R. Jin, *J. Am. Chem. Soc.,* 2008, **130**, 5883-5885.
26 D. Crasto, S. Malola, G. Brosofsky, A. Dass and H. Häkkinen, *J. Am. Chem. Soc.,* 2014, **136**, 5000-5005.
27 P. R. Nimmala and A. Dass, *J. Am. Chem. Soc.,* 2011, **133**, 9175-9177.
28 H. Qian, Y. Zhu and R. Jin, *ACS Nano*, 2009, **3**, 3795-3803.
29 G. Schmid, *Chem. Soc. Rev.*, 2008, **37**, 1909-1930.
30 P. R. Nimmala, B. Yoon, R. L. Whetten, U. Landman and A. Dass, *J. Phys. Chem. A*, 2013, **117**, 504-517.
31 P. D. Jadzinsky, G. Calero, C. J. Ackerson, D. A. Bushnell and R. D. Kornberg, *Science*, 2007, **318**, 430-433.
32 Z. Tang, D. A. Robinson, N. Bokossa, B. Xu, S. Wang and G. Wang, *J. Am. Chem. Soc.,* 2011, **133**, 16037-16044.
33 H. Qian and R. Jin, *Nano Lett.,* 2009, **9**, 4083-4087.
34 A. Desireddy, B. E. Conn, J. S. Guo, B. Yoon, R. N. Barnett, B. M. Monahan, K. Kirschbaum, W. P. Griffith, R. L. Whetten, U. Landman and T. P. Bigioni, *Nature*, 2013, **501**, 399-402.
35 S. Choi, R. M. Dickson and J. Yu, *Chem. Soc. Rev.,* 2012, **41**, 1867-1891.
36 I. Diez and R. H. A. Ras, *Nanoscale*, 2011, **3**, 1963-1970.
37 Z. Wu, E. Lanni, W. Chen, M. E. Bier, D. Ly and R. Jin, *J. Am. Chem. Soc.,* 2009, **131**, 16672-16674.
38 T. Udaya Bhaskara Rao and T. Pradeep, *Angew. Chem. Int. Ed.,* 2010, **49**, 3925-3929.
39 T. U. B. Rao, B. Nataraju and T. Pradeep, *J. Am. Chem. Soc.,* 2010, **132**, 16304-16307.
40 F. Bertorelle, R. Hamouda, D. Rayane, M. Broyer, R. Antoine, P. Dugourd, L. Gell, A. Kulesza, R. Mitrić and V. Bonačić-Koutecký, *Nanoscale*, 2013, **5**, 5637-5643.
41 X. Yuan, M. I. Setyawati, A. S. Tan, C. N. Ong, D. T. Leong and J. Xie, *NPG Asia Mater.*, 2013, **5**, e39.
42 J. Guo, S. Kumar, M. Bolan, A. Desireddy, T. P. Bigioni and W. P. Griffith, *Anal. Chem.,* 2012, **84**, 5304-5308.
43 T. Udayabhaskararao, M. Bootharaju and T. Pradeep, *Nanoscale*, 2013, **5**, 9404-9411.
44 H. Yang, J. Lei, B. Wu, Y. Wang, M. Zhou, A. Xia, L. Zheng and N. Zheng, *Chem. Commun.*, 2013, **49**, 300-302.
45 H. Yang, Y. Wang and N. Zheng, *Nanoscale*, 2013, **5**, 2674-2677.
46 G. Li, Z. Lei and Q.-M. Wang, *J. Am. Chem. Soc.*, 2010, **132**, 17670-17679.
47 S. Jin, S. Wang, Y. Song, M. Zhou, J. Zhong, J. Zhang, A. Xia, Y. Pei, M. Chen, P. Li, and M. Zhu, *J. Am. Chem. Soc.*, 2014, **136**, 15559-15565.
48 D. Fenske, C. Persau, S. Dehnen and C. E. Anson, *Angew. Chem. Int. Ed.*, 2004, **43**, 305-309.
49 C. E. Anson, A. Eichhöfer, I. Issac, D. Fenske, O. Fuhr, P. Sevillano, C. Persau, D. Stalke and J. Zhang, *Angew. Chem. Int. Ed.*, 2008, **47**, 1326-1331.
50 J. Xie, X. Jiang, Y. Zhong, Y. Lu, S. Wang, X. Wei, Y. Su and Y. He, *Nanoscale*, 2014, **6**, 9215-9222.
51 B. Sun, X. Jiang, H. Wang, B. Song, Y. Zhu, H. Wang, Y. Su and Y. He, *Anal. Chem.*, 2015, **87**, 1250-1256.
52 B. Adhikari and A. Banerjee, *Chem. Mater.,* 2010, **22**, 4364-4371.
53 X. Yuan, T. J. Yeow, Q. Zhang, J. Y. Lee and J. Xie, *Nanoscale*, 2012, **4**, 1968-1971.
54 J. Liu, X. Ren, X. Meng, Z. Fang and F. Tang, *Nanoscale*, 2013, **5**, 10022-10028.
55 J. Du, L. Jiang, Q. Shao, X. Liu, R. S. Marks, J. Ma and X. Chen, *Small*, 2013, **9**, 1467-1481.
56 I. Díez, M. Pusa, S. Kulmala, H. Jiang, A. Walther, A. S. Goldmann, A. H. Müller, O. Ikkala and R. H. Ras, *Angew. Chem. Int. Ed.,* 2009, **48**, 2122-2125.
57 E. M. Nolan and S. J. Lippard, *Chem. Rev.,* 2008, **108**, 3443-3480.
58 J. Cooper, J. A. Bolbot, S. Saini and S. J. Setford, *Water, air, and soil pollut.*, 2007, **179**, 183-195.
59 N. Cathcart, P. Mistry, C. Makra, B. Pietrobon, N. Coombs, M. Jelokhani-Niaraki and V. Kitaev, *Langmuir*, 2009, **25**, 5840-5846.
60 N. Cathcart and V. Kitaev, *J. Phys. Chem. C*, 2010, **114**, 16010-16017.
61 S. Kumar, M. D. Bolan and T. P. Bigioni, *J. Am. Chem. Soc.,* 2010, **132**, 13141-13143.
62 S. Kumar and R. Jin, *Nanoscale*, 2012, **4**, 4222-4227.
63 A. Gupta, S. K. Prajapati, M. Singh and M. Balamurugan, *Mol. Pharmaceutics*, 2007, **4**, 596-599.
64 X. Yuan, B. Zhang, Z. Luo, Q. Yao, D. T. Leong, N. Yan and J. Xie, *Angew. Chem. Int. Ed.,* 2014, **53**, 4623-4627.
65 M. Walter, J. Akola, O. Lopez-Acevedo, P. D. Jadzinsky, G. Calero, C. J. Ackerson, R. L. Whetten, H. Grönbeck and H. Häkkinen, *Proc. Natl. Acad. Sci.*, 2008, **105**, 9157-9162.
66 Z. Wu and R. Jin, *Chem. Eur. J.*, 2011, **17**, 13966-13970.
67 Z. Wu, C. Gayathri, R. R. Gil and R. Jin, *J. Am. Chem. Soc.,* 2009, **131**, 6535-6542.
68 S. J. Tan, N. R. Jana, S. Gao, P. K. Patra and J. Y. Ying, *Chem. Mater.,* 2010, **22**, 2239-2247.
69 A. R. Maity and N. R. Jana, *J. Phys. Chem. C*, 2010, **115**, 137-144.
70 B. Naim, D. Zbaida, S. Dagan, R. Kapon and Z. Reich, *The EMBO Journal*, 2009, **28**, 2697-2705.

71 S. G. Sudrik, T. Maddanimath, N. K. Chaki, S. P. Chavan, S. P. Chavan, H. R. Sonawane and K. Vijayamohanan, *Org. Lett.*, 2003, **5**, 2355-2358.
72 S. G. Sudrik, J. Sharma, V. B. Chavan, N. K. Chaki, H. R. Sonawane and K. P. Vijayamohanan, *Org. Lett.*, 2006, **8**, 1089-1092.
73 D. MacDougall and W. B. Crummett, *Anal. Chem.*, 1980, **52**, 2242-2249.
74 Z. Wu, *Angew. Chem. Int. Ed.*, 2012, **51**, 2934-2938.
75 M. Wang, Z. Wu, Z. Chu, J. Yang and C. Yao, *Chem. Asian J.*, 2014, **9**, 1006-1010.
76 C. Yao, J. Chen, M.-B. Li, L. Liu, J. Yang and Z. Wu, *Nano Lett.*, 2015, **15**, 1281-1287.
77 D. R. Lide, *CRC handbook of chemistry and physics*. CRC press: 2004.

Table of contents

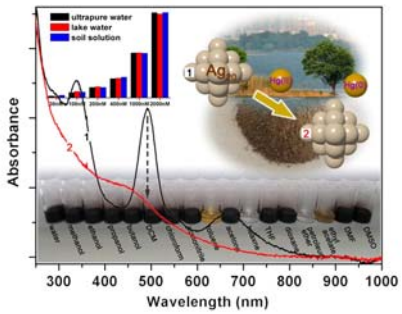

$Ag_{30}(Capt)_{18}$ was synthesized, precisely identified and employed for colorimetric probing of Hg^{2+} in environmental samples based on the AGR mechanism.